



Cite this: *Nanoscale*, 2016, **8**, 5526

## Protein source and choice of anticoagulant decisively affect nanoparticle protein corona and cellular uptake<sup>†</sup>

S. Schöttler,<sup>a,b</sup> Katja Klein,<sup>a</sup> K. Landfester<sup>a</sup> and V. Mailänder<sup>\*a,b</sup>

Protein adsorption on nanoparticles has been a focus of the field of nanocarrier research in the past few years and more and more papers are dealing with increasingly detailed lists of proteins adsorbed to a plethora of nanocarriers. While there is an urgent need to understand the influence of this protein corona on nanocarriers' interactions with cells the strong impact of the protein source on corona formation and the consequence for interaction with different cell types are factors that are regularly neglected, but should be taken into account for a meaningful analysis. In this study, the importance of the choice of protein source used for *in vitro* protein corona analysis is concisely investigated. Major and decisive differences in cellular uptake of a polystyrene nanoparticle incubated in fetal bovine serum, human serum, human citrate and heparin plasma are reported. Furthermore, the protein compositions are determined for coronas formed in the respective incubation media. A strong influence of heparin, which is used as an anticoagulant for plasma generation, on cell interaction is demonstrated. While heparin enhances the uptake into macrophages, it prevents internalization into HeLa cells. Taken together we can give the recommendation that human plasma anticoagulated with citrate seems to give the most relevant results for *in vitro* studies of nanoparticle uptake.

Received 19th November 2015,  
Accepted 9th January 2016

DOI: 10.1039/c5nr08196c

[www.rsc.org/nanoscale](http://www.rsc.org/nanoscale)

## Introduction

In the recent decade, the interest in polymeric nanocarriers for medical applications has gradually increased and accordingly a plethora of different nanoparticles have been fabricated. In particular when used as drug vectors in targeted delivery, nanocarriers could overcome many obstacles of cancer therapy. The possibility of a precise adjustment of nanocarriers' properties enables the development of specialized vectors. Nevertheless, their application is still impeded by insufficient knowledge about interactions of nanocarriers with their biological environment.

One major challenge is the rapid coverage of intravenously injected nanocarriers with blood proteins which complicates any prediction of biological outcomes.<sup>1–3</sup> This rapidly forming protein corona dramatically alters the nanocarriers' physico-chemical properties including the hydrodynamic size, surface

charge and aggregation behavior. Furthermore, the interaction with cell membranes and the mechanism of cellular uptake are controlled by the adsorbed proteins. Therefore, the corona defines the biological identity of nanoparticles, influencing cytotoxicity, body distribution and endocytosis into specific cells.<sup>4,5</sup> As it is often stated, when nanocarriers are introduced into the body, what the cells actually see is the protein corona.<sup>1</sup> Thus, the prediction of nanocarrier cell interactions is only possible if the protein corona is taken into account.

Apart from the nanocarrier surface properties, the protein corona composition is highly dependent on the biological environment. With regard to *in vitro* studies, experimental parameters such as cell culture medium,<sup>6</sup> protein concentration<sup>7</sup> and temperature<sup>8</sup> of the protein source are important factors in nanoparticle protein interactions.

Studies analyzing the protein corona of nanocarriers *in vitro* utilize different types of protein sources and many do not further specify the type used or state reasons for their choice. Serum and plasma are often used in an interchangeable manner. The origin of the protein source, *i.e.* the species from which blood was drawn or the type of anticoagulant used for plasma generation is often neglected. If the corona is determined after incubation in blood plasma, proteins of the coagulation system are often identified.<sup>9–11</sup> In contrast, serum is

<sup>a</sup>Max Planck Institute of Polymer Research, Ackermannweg 10, 55128 Mainz, Germany. E-mail: volker.mailander@unimedizin-mainz.de

<sup>b</sup>Dermatology Clinic, University Medical Center of the Johannes Gutenberg-University Mainz, Langenbeckstr. 1, 55131 Mainz, Germany

† Electronic supplementary information (ESI) available: Complete list of proteins identified by LC-MS. See DOI: 10.1039/c5nr08196c



depleted of coagulation factors. The group of Mahmoudi has reported significant variations in the protein pattern of the NP corona formed in FBS or human plasma but has not shown proteomics data.<sup>12</sup> In a second study they compared protein adsorption in human plasma samples obtained from patients with distinct diseases which also significantly affected protein composition indicating the existence of personalized protein coronas.<sup>13</sup>

The present study attempts to further contribute to a better understanding of the protein corona formation around nanocarriers in different environments as it is of great importance for the assessment of biological effects provoked by these evolving nanobioentities. For this purpose, we analyzed the impact of distinct protein sources as serum and plasma containing different anticoagulants on NP uptake and protein corona formation. The concentration of serum or plasma necessary to impair cell uptake was determined. Serum and plasma concentrations applied in cell culture affected the internalization of nanoparticles into different cell types considerably with a strong reduction of uptake at concentrations as low as 0.5%.

A major impact on protein corona composition and uptake of PS-NPs into HeLa cells and RAW267.4 macrophages was determined for distinct protein sources such as FBS, human serum and human plasma. A strong uptake of nanoparticles coated with FBS was observed for both cell lines, while human serum and human citrate plasma impair NP internalization. The most exciting finding was the opposing uptake of particles incubated in human heparin plasma. While the particles were internalized by macrophages, no uptake was observed for HeLa cells. Further experiments proved that heparin is responsible for this effect.

These significant implications on NP cell interactions induced by the characteristics of the surrounding environment underline the importance of a careful choice of experiment parameters for *in vitro* protein corona analysis. Highlighting these effects elicited by different protein sources is crucial to ensure the comparability of studies and important information can be gained for future studies.

## Results

### Influence of the protein source and cell type on NP uptake

As several studies have reported that for distinct nanoparticles the cell interaction is diminished when proteins are present in the cell culture medium compared to conditions where no proteins are present, we first determined what concentration of protein containing supplement is necessary to decrease the uptake. Therefore, a model monodisperse, fluorescently labeled, amino-functionalized polystyrene nanoparticle with a diameter of 106 nm was prepared by miniemulsion polymerization (PS-NH<sub>2</sub>) and its uptake into HeLa cells was analysed by flow cytometry, comparing the interaction of nanoparticles and cells cultured in different concentrations of human serum and human heparin plasma (Fig. 1). The cells were cultured in serum-free medium for 2 h before the medium was

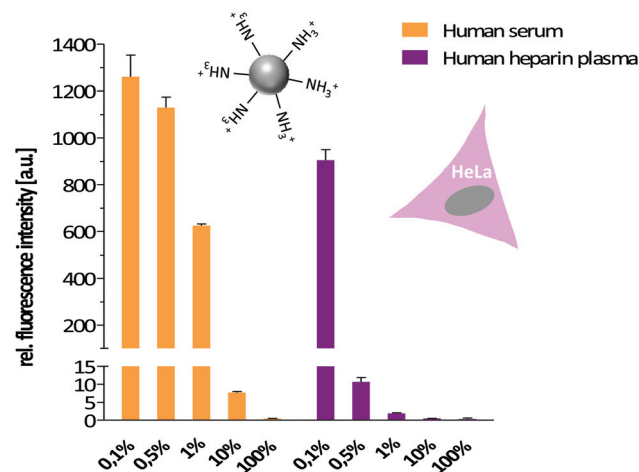


**Fig. 1** Impact of human serum and plasma on uptake of PS-NH<sub>2</sub> into HeLa cells. Cellular uptake of PS-NH<sub>2</sub> nanoparticles into HeLa cells cultured in medium containing 0.1 to 100% of either human serum (orange) or human heparin plasma (purple) was analysed by flow cytometry after 2 h incubation. Values are expressed as mean  $\pm$  SD of triplicates.

changed to the indicated protein source concentrations and the particles were added. The serum dilution reveals that uptake of PS-NH<sub>2</sub> is already reduced by 50% with only 1% serum present in the cell culture medium. The cells cultured in a medium containing more than 1% serum barely internalize any NPs. For human heparin plasma the effect is even stronger. Only 0.5% plasma is enough to reduce the uptake by 98.8%. While the protein composition in serum has been changed by activating the proteins of the coagulation cascade and ultimately removing *e.g.* fibrinogen, we expected that anticoagulated plasma with different anticoagulants will have no varying effect on cell uptake. Surprisingly, there was not only a remarkable difference between distinct sera (FBS *versus* human serum (HS)), but also between differently anticoagulated plasmas (Fig. 2). While fetal bovine serum (FBS), the most common protein source in cell culture, leads to a strong uptake, human serum (HS) does not allow a detectable uptake in HeLa cells (Fig. 2a) or even a macrophage cell line (RAW 264.7, Fig. 2b). This can be explained by the fact that FBS is additionally heat inactivated while human serum (HS) is not (see Lesniak *et al.*<sup>14</sup>).

Most intriguingly human heparin plasma (HHP) and human citrate plasma (HCP) showed a significant difference with more uptake in HeLa cells for HCP (Fig. 2a) while this was completely reversed for the macrophage cell line (Fig. 2b) with a strong uptake for HHP.

The strong difference in cellular uptake of NPs incubated in various types of protein sources displayed in Fig. 2 raised the question whether the effect is triggered by a distinct protein adsorption pattern of specific proteins. Thus, the composition of the protein corona was further analysed by SDS-PAGE and quantitative proteomics with liquid chromatography-mass spectrometry (LC-MS).



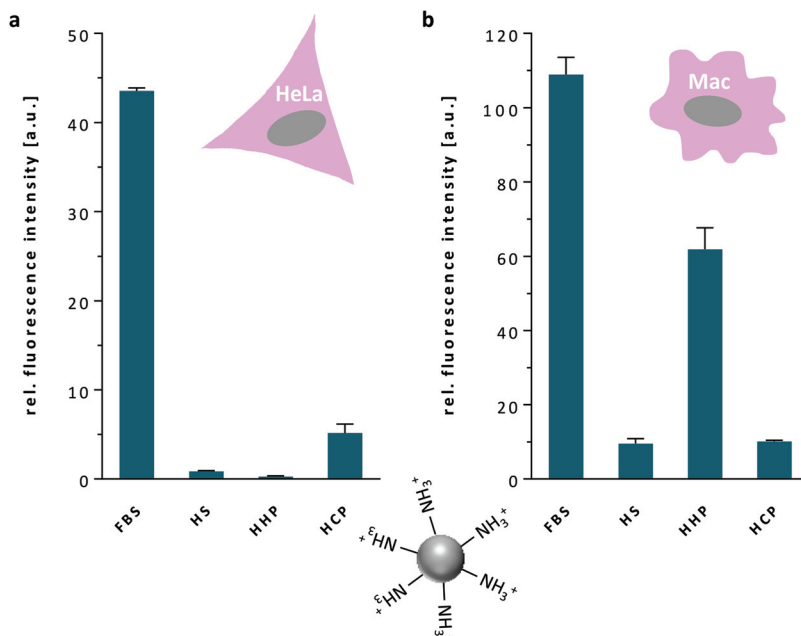


**Fig. 2** Influence of different protein sources on uptake of PS-NH<sub>2</sub> into HeLa cells and macrophages. Uptake of PS-NH<sub>2</sub> into (a) HeLa cells after 4 h incubation and into (b) RAW264.7 macrophages after 2 h incubation analysed by flow cytometry. Cells were cultured in serum-free medium for 2 h before cell medium was changed to 100% fetal bovine serum (FBS), human serum (HS), human heparin plasma (HHP) or human citrate plasma (HCP) directly before NP addition. Values are expressed as mean  $\pm$  SD of triplicates.

### Investigation of the protein corona composition of different protein sources and anticoagulants

A comparison of hard corona proteins formed around PS-NH<sub>2</sub> in FBS, HS, HHP and HCP after separation by centrifugation is depicted in Fig. 3 (for soft *versus* hard corona see ref. 15). The amount of adsorbed proteins was quantified by a colorimetric protein assay (Fig. 3a). The strongest protein adsorption was observed in HCP, followed by HHP and HS. The lowest protein concentration was measured for the FBS samples. The SDS-PAGE in Fig. 3b shows that the strongest difference in the protein pattern is seen between FBS and the human samples. In addition to the strong albumin band (just above the 62 kDa marker), the plasma samples (HHP and HCP) exhibit bands which could be attributed to fibrinogen (see proteomics results below). Fibrinogen consists of three subunits, the alpha, beta, and gamma chain, detected at 47, 56, and 63 kDa, respectively. Here also the high reproducibility of the method is visually demonstrated by the similarity of the protein pattern between the three replicates for each protein source.

To further analyze the protein corona samples, label-free quantitative proteomics by LC-MS analysis was performed. In total 290 proteins were identified for all samples (4 conditions, 3 biological replicates, 3 technical replicates). The complete list of identified proteins is shown in Tables S1 and S2.† Fig. 4 outlines the composition of the different protein coronas around PS-NH<sub>2</sub>; the majority of proteins was only identified in very low concentrations and is thus expressed as “Others”. As already suggested by SDS-PAGE, albumin is the major protein

in all samples. It accounts for 58% of the protein corona formed in human serum, 46% in the FBS corona and 47% and 39% in the coronas formed in human heparin and citrate plasma, respectively. Furthermore, the plasma samples contain considerable amounts of fibrinogen. Adding up the percentages determined for the three subunits, fibrinogen has a 39% share in the corona formed in citrate plasma and 22% in heparin plasma. Additionally, vitronectin and clusterin were identified as abundant proteins on the NPs after incubation in all three human samples. With 19% the highest amount of clusterin was determined for the human serum samples, whereas the same amount of vitronectin was adsorbed to the particles in heparin plasma. Interestingly, incubation with FBS leads to a strong adsorption of (pro)thrombin and hemoglobin, although these proteins are not very abundant in pure FBS.

In conclusion, a significant difference between the bovine and human samples was detected. This could explain the increased uptake of PS-NH<sub>2</sub> incubated in FBS for both tested cell types (Fig. 2), especially as a high abundance of (pro)thrombin on the particle surface has already been linked to an increased cell interaction.<sup>11</sup> Additionally, the overall lower protein adsorption in FBS (Fig. 3) points towards an enhanced cell uptake. NPs incubated in human serum bind a higher amount of clusterin compared to particles incubated in FBS. This suggests a participation of clusterin in reducing the uptake of PS-NH<sub>2</sub> incubated in human serum into HeLa cells and macrophages.<sup>16</sup> Despite these conclusive results, the protein patterns formed around the nanocarrier in citrate and



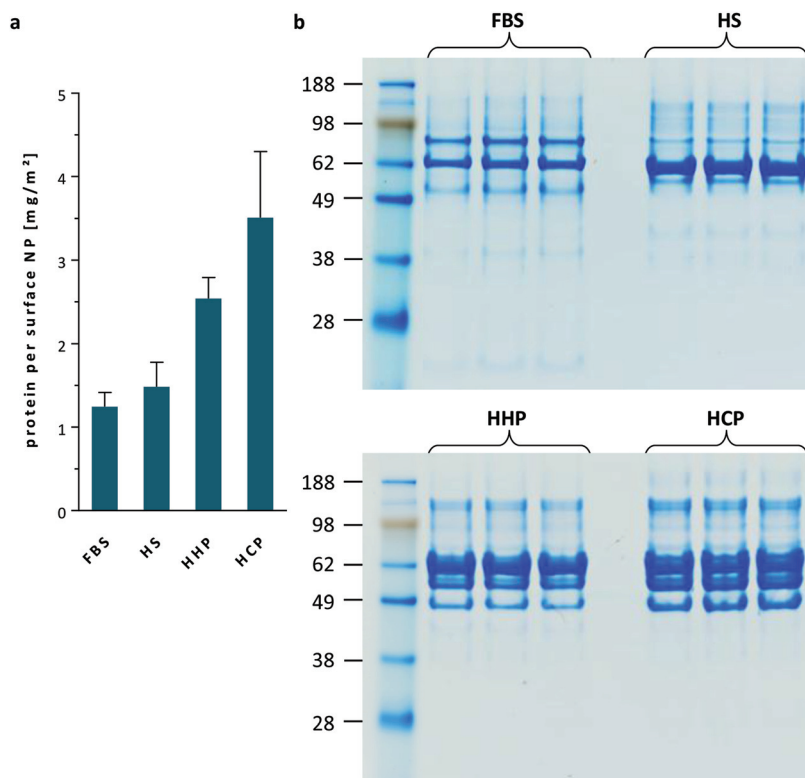


**Fig. 3** Protein adsorption to the surface of PS-NH<sub>2</sub> NPs after incubation in different protein sources. PS-NH<sub>2</sub> NPs were incubated with FBS, human serum (HS), human heparin plasma (HHP) or human citrate plasma (HCP) for 1 h at 37 °C and hard corona proteins were prepared by centrifugation. (a) Quantification of adsorbed proteins with Pierce 660 nm assay in mg protein per NP surface area (m<sup>2</sup>). Values are expressed as mean  $\pm$  SD of the three biological replicates. (b) SDS-PAGE was used to visualize the protein corona (PC) composition formed around PS-NH<sub>2</sub> NPs in the different protein sources. To guarantee reproducibility, the analysis was performed in triplicates.

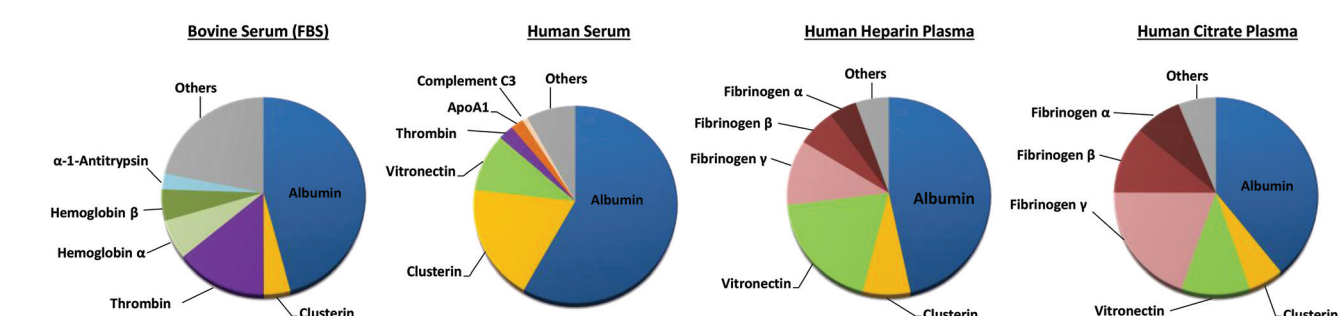


**Fig. 4** Composition of the protein corona of PS-NH<sub>2</sub> NPs after incubation with FBS, HS, HHP or HCP determined by quantitative LC-MS. Mean values were calculated from the molar masses of each protein for three biological and three technical replicates. Only the six most abundant proteins of each protein corona are shown separately, the amount of remaining proteins was summed up as others.

heparin plasma display a high level of similarity. The prominent difference in macrophage uptake of PS-NH<sub>2</sub> incubated in the two plasma types can thus not be explained adequately by protein adsorption. The results suggest that besides protein corona formation the type of anticoagulant used for plasma generation might play a major role in cell interaction and was further examined.

#### Effect of the anticoagulant heparin

As no strong difference between the compositions of the different protein coronas on PS-NH<sub>2</sub> in the two investigated plasma samples was detected, the part played by the polysaccharide heparin in nanoparticle-cell interaction was explored. The highest uptake of the amino functionalized particle was

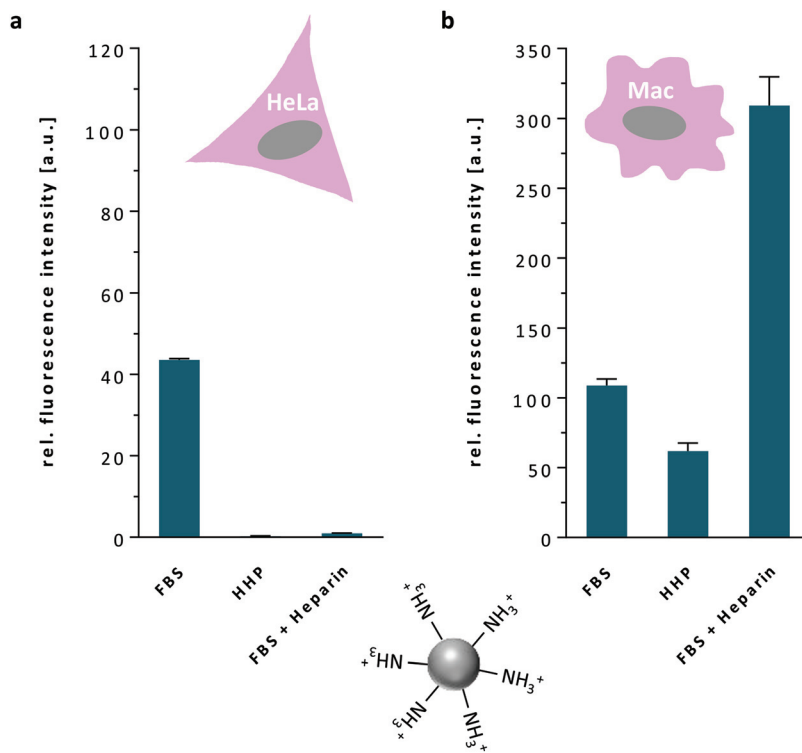


**Fig. 5** Influence of heparin on uptake of PS-NH<sub>2</sub> into HeLa cells and macrophages. Uptake of PS-NH<sub>2</sub> into (a) HeLa cells after 4 h incubation and into (b) RAW264.7 macrophages after 2 h incubation analysed by flow cytometry. Cells were cultured in serum-free medium for 2 h before cell medium was changed to 100% fetal bovine serum (FBS), human heparin plasma (HHP) or FBS supplemented with heparin (17 IU ml<sup>-1</sup>) directly before NP addition. Values are expressed as mean  $\pm$  SD of triplicates.

detected for FBS for both investigated cell lines. Therefore, FBS was used as a reference to monitor the effect of heparin. Fig. 5 shows the uptake of PS-NH<sub>2</sub> into HeLa cells and macrophages maintained in FBS or heparin plasma as already seen in Fig. 2, but this time the cells were additionally incubated in FBS supplemented with heparin. Heparin was added at the same concentration (17 IU ml<sup>-1</sup>) as commonly applied in BD Vacutainer® Plasma Tubes for heparin plasma generation. Strikingly, uptake of PS-NH<sub>2</sub> in FBS containing heparin was almost completely inhibited compared to uptake in pure FBS. The internalization is reduced to the same extent as by heparin plasma. In contrast, the mixture of FBS and heparin strongly enhances the uptake into macrophages (Fig. 5b). This is in agreement with the fact that uptake of the particles incubated in heparin plasma is also significantly higher than for particles in human serum or citrate plasma.

At this point, there are a number of different scenarios for the role played by heparin. For instance, the polysaccharide could either adsorb to the nanoparticles or directly bind to the cells and alter the cellular behavior without being adsorbed to the nanoparticle. In order to pinpoint this question, in a next step the particles were either incubated with FBS alone or FBS supplemented with heparin (Fig. 6). Unbound proteins and heparin were then removed by centrifugation and the coated NPs were added to HeLa cells, thus no free heparin was present. Additionally, the FBS coated particles were added to

the cells cultured in a medium containing heparin. It was assumed that in this way a distinction between the interaction of heparin with the particles and an interaction with the cells was possible. Nevertheless, in both cases, uptake of PS-NH<sub>2</sub> was prevented. NPs pre-coated with FBS and subsequently added to cells cultured in a medium containing heparin and NPs coated with FBS and heparins were not internalized by HeLa cells.

These intriguing results raised further questions. Can heparin alone inhibit particle uptake or are the proteins present in FBS necessary for the effect? This question was addressed in the following experiment depicted in Fig. 7. First, PS-NH<sub>2</sub> particles were added to HeLa cells cultured in a cell culture medium without proteins, a cell culture medium containing FBS alone, and a cell culture medium containing heparin alone or both (Fig. 7a). The flow cytometry analysis shows that only the combination of FBS and heparin prevents the uptake of particles into HeLa cells. Heparin alone does not have a significant effect on particle internalization.

Does heparin prevent endocytosis of HeLa cells in general? Therefore the uptake of AF488-dextran was analysed under the same conditions. Tracing the internalization of fluorescent dextran is a standard method to monitor endocytosis. Fig. 7b illustrates that heparin has no influence on dextran uptake. Thus heparin does not prevent macropinocytosis of HeLa cells in general but only affects nanoparticle uptake while it seems



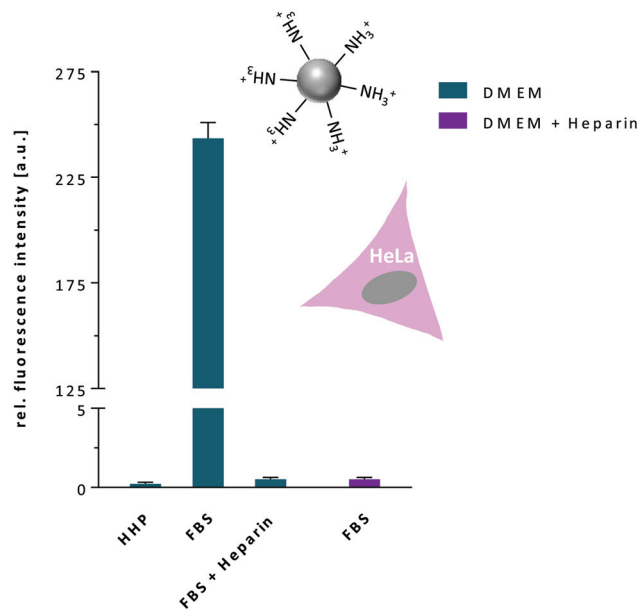


**Fig. 6** Uptake of PS-NH<sub>2</sub> into HeLa cells after incubation with HHP, FBS or FBS and heparin (17 IU ml<sup>-1</sup>). NPs were incubated with protein sources for 1 h at 37 °C and centrifuged to remove residual proteins before NPs were added to cells cultured in pure DMEM (green) or DMEM supplemented with heparin (17 IU ml<sup>-1</sup>; purple). Uptake was analysed by flow cytometry after 2 h incubation. Values are expressed as mean  $\pm$  SD of triplicates.

to be adsorbed to the nanoparticle. Considering these two results together we conclude that heparin alters the uptake of cargo when it is bound to the surface of the cargo, *i.e.* the nanoparticle.

## Discussion

This study addresses several parameters which are often neglected when analyzing interactions of nanocarriers, proteins and cells, such as protein concentration, protein source, different anticoagulants and cell type. Our results reveal important differences for the protein corona formation and NP uptake dependent on the protein source, emphasizing that the formation of different bionanostructures exerts different biological effects.

The results presented indicate that, in general, proteins attenuate the uptake of polystyrene nanoparticles into cells. Related results have been reported by Lesniak *et al.*, showing a reduced uptake of polystyrene nanoparticles when proteins are present in the cell culture medium.<sup>17</sup> Furthermore, we show that the concentration of the protein source has deep implications on particle uptake. Serum and plasma concentrations as low as 0.5% already have a major impact by strongly reducing the internalization of an amino-functionalized polystyrene nanoparticle into HeLa cells. This should be taken into

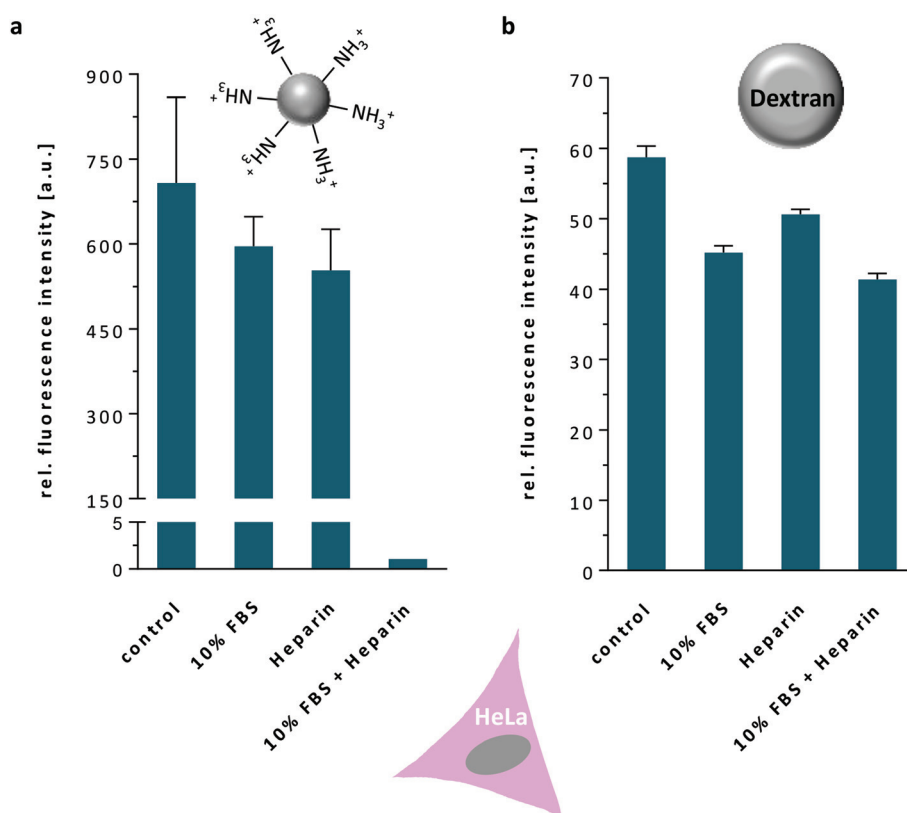


**Fig. 7** Effects of heparin on uptake of PS-NH<sub>2</sub> and dextran into HeLa cells. Uptake of (a) PS-NH<sub>2</sub> and (b) AF488-dextran (100  $\mu$ g ml<sup>-1</sup>) into HeLa cells was analysed by flow cytometry after 2 h incubation. Cells were cultured in serum-free medium for 2 h before cell medium was changed to pure DMEM (control), DMEM containing either 10% FBS, heparin (17 IU ml<sup>-1</sup>) or both. Values are expressed as mean  $\pm$  SD of duplicates.

account in all experiments investigating cellular uptake of nanocarriers. In order to adjust *in vitro* experiments to be as close as possible to *in vivo* conditions, it should be considered to use 100% of the respective protein source as this is the natural concentration *in vivo*. However, no large discrepancies between 10%, the concentration most commonly used for cell culture experiments, and 100% were observed for particle cell interactions.

Most importantly, it was demonstrated that the choice of the protein source is crucial for nanoparticle uptake analysis. Many recent studies of great importance investigating the different aspects of the protein corona of nanocarriers employed different protein sources as FBS,<sup>17,18</sup> human serum,<sup>19,20</sup> human citrate<sup>3,21</sup> or EDTA plasma<sup>2,22</sup> without further stating reasons for their choice. The results shown here emphasize the necessity of a careful decision concerning the protein source as the outcome of experiments is strongly dependent on it.

Hard corona protein profiles varied significantly between the investigated protein sources: FBS, human serum, human heparin and citrate plasma. A strong difference in corona composition was especially prominent between the human and bovine media. As FBS is the most frequently used supplement for many cells cultured *in vitro*, it is also often employed in protein corona studies. But in order to obtain a significant improvement in the prediction of the *in vivo* fate of nanoparticles, it is important to test the protein corona formation in the respective medium *i.e.* the exact protein source of the desired species (*e.g.* murine or human) before applying nanocarriers *in vivo*.

Furthermore, the distinction between plasma and serum is often neglected. A rather strong adsorption of fibrinogen to nanoparticles from both plasma samples was observed and might affect nanoparticle uptake substantially. As fibrinogen is not present at large in serum as it has been clotted to fibrin, this is a huge and important difference. Thus the distinction should not be ignored.

On the other hand, anticoagulants used for plasma generation can bias the observations significantly. During plasma preparation from whole blood, blood clotting is prevented either by EDTA, citrate or heparin. EDTA and citrate are both effective by calcium complexation and thus do not change the protein composition. Heparin binds to antithrombin III (ATIII) and increases its activity in blocking thrombin and therefore inhibits fibrin clot formation. Most importantly ATIII is not detected or below 1% of total protein of the protein corona formed for the plasma samples.

In their publication analyzing the uptake of polystyrene nanoparticles into different types of white blood cells Baumann *et al.* have already described the influence of EDTA on endocytosis.<sup>23</sup> They report a dramatically reduced uptake of carboxy and amino-functionalized nanoparticles into CD14+ monocytes and CD16+ neutrophil granulocytes when EDTA or citrate was used instead of heparinized blood. Therefore, it was concluded that EDTA is hindering the uptake by complexing calcium, as calcium is needed as a signaling messenger in phagocytosis.

The present study further investigates the effect of heparin and it was shown that heparin enhances uptake into macrophages and even more strikingly inhibits the uptake of nanoparticles into HeLa cells. Heparin is a natural glycosaminoglycan composed of repeating disaccharide units consisting of uronic acid and D-glucosamine. It is most commonly known as an anticoagulant and has been used as a drug since the 1930s. In addition to its well investigated anticoagulant activity, heparin is involved in diverse physiological processes including cell proliferation, differentiation, inflammation, angiogenesis and viral infectivity through interacting with a large range of proteins.<sup>24</sup> It also exerts anticancer activities in the processes of tumor progression and metastasis.<sup>25</sup> Still, usually heparin is stored within the secretory granules of mast cells and released only into the vasculature at sites of tissue injury.<sup>24</sup> With its high content of sulpho and carboxyl groups, heparin has the highest negative charge density of any known biological molecule.<sup>26</sup>

Binding of highly negatively charged heparin to the nanoparticle surface might cause an unfavorable interaction between the nanoparticles and the negatively charged cell membrane. Accordingly, numerous studies have shown that the surface charge has a significant impact on cellular internalization of a variety of nanocarriers. Positively charged nanoparticles reveal a high rate of internalization into HeLa cells, whereas negatively charged NPs exhibit a poor rate of endocytosis.<sup>27-29</sup>

Nevertheless, reported effects of heparin on cellular uptake of nanomaterials are quite controversial. As heparin has been shown to inhibit complement activation,<sup>30-32</sup> binding of heparin to surfaces has been suggested as an alternative for PEGylation in a biomimetic approach. Heparin immobilized to the surface of nanocarriers can mimic eukaryotic cells that are naturally covered with glycosaminoglycans, thus concealing the unnatural nanoparticles from the immune system. Accordingly, several manuscripts report a prolonged blood circulation of nanoparticles coated with heparin.<sup>33-35</sup> Furthermore, heparin has proven its ability to inhibit the adsorption and the internalization of nanoparticles by a murine macrophage-like cell line *in vitro*.<sup>36</sup>

On the other hand, a high uptake of heparin-based nanocapsules into different tumor cell lines was described,<sup>37</sup> as well as an enhanced uptake of heparin functionalized PLGA-based nanoparticles into a fibroblast and tumor cell line.<sup>38</sup> In our study we have seen an enhanced uptake into macrophages when heparin is present, but an inhibition into the cancer cell line HeLa. Clearly the difference between these approaches and ours is the type of cell used and also the way the heparin has been bound or in our case adsorbed to the particles.

Up to now, the mechanism of this process is unclear. Interestingly, proteins seem to be necessary for this effect as heparin alone does not prevent the uptake of PS-NPs into HeLa cells. Proteins present in FBS are sufficient to provoke the reduced uptake and the high amount of coagulation proteins only present in plasma is not necessary. Furthermore, it was shown that heparin does not impair the internalization of



dextran by HeLa cells indicating that a specific interaction of heparin and the nanocarriers occurs and the adsorbed heparin leads to decreased uptake while endocytosis by heparin in medium is not inhibited in general.

The opposing effects of heparin on NP uptake by HeLa cells and macrophages point to the different mechanisms of entry into various cells. Different ways of endocytosis utilized by non-phagocytic cells as HeLa and phagocytes like macrophages seem to be relevant for the effect provoked by heparin. Already in 1983, Bleiberg *et al.*<sup>39</sup> postulated heparin receptors on mouse macrophages and evidence for a scavenger mediated uptake into the same macrophage-like cell line used in the present study (RAW264.7) was published by Falcone six years later.<sup>40</sup> Matching *in vivo* data further linked liver uptake of heparin to a scavenger receptor mediated mechanism.<sup>41</sup> Furthermore, Lindstedt *et al.* showed that soluble heparin proteoglycans secreted by stimulated mast cells trigger uptake of LDL by macrophages through scavenger receptor-mediated phagocytosis.<sup>42</sup> All these reports provide evidence that heparin's binding to RAW264.7 cells is mediated by the scavenger receptors and fit the high uptake of nanoparticles incubated with heparin plasma or FBS supplemented with heparin into macrophages.

Laurent *et al.* have already pointed out the key role of the protein source in the formation of the associated protein corona and the impact of the cell "observer" effect.<sup>12</sup> They compared the corona composition formed around superparamagnetic iron oxide nanoparticles (SPIONs) in FBS and human plasma (the anticoagulant was not further specified) with SDS-PAGE and determined significant differences. Furthermore, cell uptake and toxicity were probed for various cell lines and the results indicate that each cell type responds differently to the nanoparticles. Nevertheless, they did not analyze the combined effect of the distinct protein sources and the cell types.

## Experimental

### Nanoparticle preparation and characterization

The polystyrene nanoparticles were prepared using a modified protocol as previously described.<sup>43</sup> A macroemulsion was prepared with a continuous phase containing cetyltrimethylammonium chloride solution (CTMA-Cl) (25 wt% in water, 400 mg,  $3.1 \times 10^{-4}$  mol) as the surfactant and 2-aminoethyl methacrylate hydrochloride (AEMH) (180 mg,  $1.1 \times 10^{-3}$  mol, 3 wt% to styrene, for the introduction of amino functionalities) in 23.6 g Millipore water and a dispersed phase containing distilled styrene (5.88 g,  $5.7 \times 10^{-2}$  mol), hexadecane (251 mg,  $1.1 \times 10^{-3}$  mol) as the hydrophobe, Bodipy methacrylate (9.6 mg,  $2.1 \times 10^{-5}$  mol) as the fluorescent dye and 2,2'-azobis (2-methylbutyronitrile) (V59) (100 mg,  $5.2 \times 10^{-4}$  mol) as the oil soluble azo initiator.

Both phases were made homogeneous by mechanical stirring and the continuous phase was added slowly to the stirring dispersed phase. The macroemulsion was stirred for 1 h at the highest speed. Subsequently, the macroemulsion

was ultrasonicated with a Branson Sonifier (1/2" tip, 6.5 nm diameter) for 2 min at 450 W 90% amplitude under ice cooling to obtain a miniemulsion. The miniemulsion was directly transferred into a 50 mL flask and stirred in an oil bath at 72 °C. The polymerization was run for 18 h. The dispersion was purified by centrifugation (2.5 h, 12 000 rpm; 3 times), the supernatant was always removed and the pellet redispersed in sterile water.

A hydrodynamic particle diameter of 116 nm ( $\pm 13$  nm) was determined using a NICOMP zetasizer (Agilent Technologies). The measurement was conducted at 25 °C in a diluted aqueous dispersion at an angle of 90°. Zeta potential measurements were performed with a Malvern Instruments Zeta Nanosizer at a detection angle of 173° in a  $10^{-3}$  M KCl sample dispersion. A  $\xi$ -potential of 42.8 mV was determined for the amino functionalized polystyrene nanoparticles.

### Plasma and serum samples

Whole blood was taken at the Department of Transfusion Medicine Mainz from healthy donors after physical examination and after obtaining informed consent in accordance with the Declaration of Helsinki. For human serum generation, blood was clotted overnight according to a standard procedure and serum from seven volunteers was pooled into one batch. Plasma was generated by addition of either citrate (0.2 ml CPD solution per ml) or Na-heparin (20 IU ml<sup>-1</sup>) as anticoagulants and subsequent centrifugation. Human heparin and citrate plasma from ten and six donors, respectively, was pooled into one batch and all samples were stored at -80 °C. With Pierce 660 nm protein assay a protein concentration of 69 mg ml<sup>-1</sup> was determined for human serum, 66 mg ml<sup>-1</sup> for human heparin and citrate plasma. To remove any aggregated proteins the samples were centrifuged for 1 h at 20 000g before usage.

### Cell culture

Human cervix carcinoma cells (HeLa) and the murine macrophage cell line RAW264.7 were cultured in Dulbecco's modified eagle medium (DMEM), supplemented with 10% FCS, 100 U per ml penicillin, 100 mg per ml streptomycin and 2 mM glutamine. All cells were grown in a humidified incubator at 37 °C and 5% CO<sub>2</sub>.

For the uptake experiments, the cells were seeded at a density of 20 000 cells per cm<sup>2</sup>. For the analysis of nanoparticle internalization under serum-free conditions, the cells were washed 3 times with PBS and incubated in fresh serum-free medium for 2 h before the cell medium was exchanged for 100% fetal bovine serum (FBS), human serum (HS), human heparin plasma (HHP), human citrate plasma (HCP) or FBS supplemented with heparin (Rotexmedica). Nanoparticle dispersions were added at a concentration of 75 µg ml<sup>-1</sup> to the cells and dextran labeled with Alexa Fluor® 488 (Thermo Fisher Scientific) was added at a concentration of 100 µg ml<sup>-1</sup>. Before the cells were analysed by flow cytometry they were washed to remove free nanoparticles.



## Flow cytometry

For the quantitative analysis of nanoparticle uptake into cells flow cytometry measurements were conducted. After the indicated incubation time, adherent cells were washed with DPBS and subsequently detached from the culture vessel with 2.5% trypsin. Flow cytometry measurements were performed on a CyFlow ML cytometer with a 488 nm laser for excitation of Bodipy-1 and a 527 nm band pass filter for emission detection. Data analysis was performed using FCS Express V4 software by selecting the cells on a forward/sideward scatter plot, thereby excluding cell debris. These gated events were further analysed by the amount of fluorescence signal expressed as a median intensity. The median intensity of a negative control was subtracted from the obtained values. Mean values and standard deviation were determined from triplicates.

## Protein corona preparation

To ensure reproducibility the ratio of total particle surface area to plasma concentration was kept at  $20 \text{ ml m}^{-2}$ . The nanoparticle dispersion was diluted with ultrapure water to a constant particle surface concentration ( $0.05 \text{ m}^2$  in  $300 \mu\text{L}$ ) and this dispersion was incubated with 1 ml plasma or serum for 1 h at  $37^\circ\text{C}$  with constant agitation. The incubation time was chosen because previous reports confirmed that the protein corona is formed in a relatively stable manner over a period of 1 h.<sup>1</sup> The nanoparticles were separated from the supernatant by centrifugation at  $20\,000\text{g}$  for 1 h. The particle pellet was resuspended in PBS and washed by three centrifugation steps at  $20\,000\text{g}$  for 1 h and subsequent redispersion in PBS. Before the last washing step, the dispersion was transferred into a fresh protein Lobind tube. Proteins were eluted from the particles by dissolving the particle–protein pellet in  $300 \mu\text{l}$  urea–thiourea buffer (7 M urea, 2 M thiourea, 4% CHAPS). Protein concentrations were determined using Pierce 660 nm protein assay according to manufacturer's instructions with BSA as a standard.

## SDS PAGE

For SDS PAGE  $16.25 \mu\text{l}$  of the protein sample was mixed with  $6.25 \mu\text{l}$  NuPAGE LDS sample buffer and  $2.5 \mu\text{l}$  NuPAGE sample reducing agent and loaded onto a NuPAGE 10% bis–tris protein gel. The electrophoresis was carried out in NuPAGE MES SDS running buffer at  $150 \text{ V}$  for 1.5 h with SeeBlue Plus2 Pre-Stained Standard as a molecular marker. The gel was stained using SimplyBlue SafeStain according to the instruction manual.

## Liquid-chromatography mass-spectrometry (LC-MS) analysis

Proteins were digested by following the protocol of Hofmann *et al.*<sup>44</sup> with few modifications. Briefly,  $25 \mu\text{g}$  of each protein sample were precipitated using the ProteoExtract protein precipitation kit according to the supplier's manual. The protein pellet was resuspended in  $100 \mu\text{l}$  0.1% RapiGest SF in  $50 \text{ mM}$  ammonium bicarbonate and incubated for 15 min at  $80^\circ\text{C}$ . Dithiothreitol was added to a final concentration of  $5 \text{ mM}$

before the sample was incubated at  $56^\circ\text{C}$  for 45 min. Iodoacetamide was added to a final concentration of  $15 \text{ mM}$  and the samples were kept for 1 h in the dark. Proteins were digested overnight at  $37^\circ\text{C}$  using trypsin with an enzyme to protein ratio of 1 : 50. To stop the enzymatic digestions and to degrade RapiGest SF  $2 \mu\text{l}$  hydrochloric acid were added and the sample was incubated for 45 min at  $37^\circ\text{C}$ . To remove water immiscible degradation products of RapiGest SF, the sample was centrifuged at  $13\,000\text{g}$ , for 15 min. For LC-MS analysis the samples were diluted 10-fold with aqueous  $0.1\%$  formic acid and spiked with  $50 \text{ fmol } \mu\text{l}^{-1}$  Hi3 Ecoli Standard (Waters Corporation) for absolute quantification.

Quantitative analysis of protein samples was performed using a nanoACQUITY UPLC system coupled with a Synapt G2-Si mass spectrometer. Tryptic peptides were separated on the nanoACQUITY system equipped with a C18 analytical reversed-phase column ( $1.7 \mu\text{m}$ ,  $75 \mu\text{m} \times 150 \text{ mm}$ ) and a C18 nanoACQUITY trap column ( $5 \mu\text{m}$ ,  $180 \mu\text{m} \times 20 \text{ mm}$ ). Samples were processed with mobile phase A consisting of  $0.1\%$  (v/v) formic acid in water and mobile phase B consisting of acetonitrile with  $0.1\%$  (v/v) formic acid. The separation was performed at a sample flow rate of  $0.3 \mu\text{l min}^{-1}$ , using a gradient of 2–37% mobile phase B over 70 min. As a reference compound  $150 \text{ fmol } \mu\text{l}^{-1}$  Glu-Fibrinopeptide was infused at a flow rate of  $0.5 \mu\text{l min}^{-1}$ .

Data-independent acquisition ( $\text{MS}^{\text{E}}$ ) experiments were performed on the Synapt G2-Si operated in resolution mode. Electrospray ionization (ESI) was performed in positive ion mode using a NanoLockSpray source. Data was acquired over a range of  $m/z$  50–2000 Da with a scan time of 1 s, ramped trap collision energy from 20 to 40 V with a total acquisition time of 90 min. All samples were analysed in triplicates. Data acquisition and processing were carried out using MassLynx 4.1.

## Data processing and protein identification

Progenesis QI for proteomics was used to process data and identify peptides. Continuum LC-MS data were post acquisition lock mass corrected. Noise reduction thresholds for low energy, high energy and peptide intensity were fixed at 120, 25, and 750 counts, respectively. During database searches, the protein false discovery rate was set at 4%. The generated peptide masses were searched against a reviewed human protein sequence database downloaded from Uniprot. For samples originating from FBS a reviewed bovine database was used. Sequence information of Hi3 Ecoli standard (chaperone protein ClpB) was added to the database to conduct absolute quantification.<sup>45,46</sup> The following criteria were used for the search: one missed cleavage, maximum protein mass 600 kDa, fixed carbamidomethyl modification for cysteine and variable oxidation for methionine. For identification a peptide was required to have at least three assigned fragments and a protein was required to have at least two assigned peptides and five assigned fragments. Identified peptides with score parameters less than 4 were generally rejected. Quantitative data were generated based on the TOP3/Hi3 approach, providing the amount of each protein in fmol.<sup>47</sup>



## Conclusions

The results presented here, prove that the same protein source can have a very different impact on distinct cell types and that not only serum *versus* plasma is important but also the influence of the employed anticoagulant is of utmost importance and a factor which should be taken into account. From our results citrate anticoagulated plasma seems to be the best source of plasma in regard to adsorption of plasma proteins onto surfaces without which the anticoagulant itself would have an influence on cell uptake.

## Acknowledgements

The authors wish to thank the Deutsche Forschungsgemeinschaft (DFG, SFB1066, Project Q2 and B9) for supporting the study. The Max Planck society is gratefully acknowledged.

## Notes and references

- 1 D. Walczyk, F. B. Bombelli, M. P. Monopoli, I. Lynch and K. A. Dawson, *J. Am. Chem. Soc.*, 2010, **132**, 5761–5768.
- 2 T. Cedervall, I. Lynch, S. Lindman, T. Berggard, E. Thulin, H. Nilsson, K. A. Dawson and S. Linse, *Proc. Natl. Acad. Sci. U. S. A.*, 2007, **104**, 2050–2055.
- 3 S. Tenzer, D. Docter, J. Kuharev, A. Musyanovych, V. Fetz, R. Hecht, F. Schlenk, D. Fischer, K. Kiouptsi, C. Reinhardt, K. Landfester, H. Schild, M. Maskos, S. K. Knauer and R. H. Stauber, *Nat. Nanotechnol.*, 2013, **8**, 772–781.
- 4 C. D. Walkey and W. C. Chan, *Chem. Soc. Rev.*, 2012, **41**, 2780–2799.
- 5 E. Hellstrand, I. Lynch, A. Andersson, T. Drakenberg, B. Dahlback, K. A. Dawson, S. Linse and T. Cedervall, *FEBS J.*, 2009, **276**, 3372–3381.
- 6 G. Maiorano, S. Sabella, B. Sorce, V. Brunetti, M. A. Malvindi, R. Cingolani and P. P. Pompa, *ACS Nano*, 2010, **4**, 7481–7491.
- 7 M. Ghavami, S. Saffar, B. Abd Emamy, A. Peirovi, M. A. Shokrgozar, V. Serpooshan and M. Mahmoudi, *RSC Adv.*, 2013, **3**, 1119–1126.
- 8 M. Mahmoudi, A. M. Abdelmonem, S. Behzadi, J. H. Clement, S. Dutz, M. R. Ejtehadi, R. Hartmann, K. Kantner, U. Linne, P. Maffre, S. Metzler, M. K. Moghadam, C. Pfeiffer, M. Rezaei, P. Ruiz-Lozano, V. Serpooshan, M. A. Shokrgozar, G. U. Nienhaus and W. J. Parak, *ACS Nano*, 2013, **7**, 6555–6562.
- 9 M. Gasser, B. Rothen-Rutishauser, H. Krug, P. Gehr, M. Nelle, B. Yan and P. Wick, *J. Nanobiotechnol.*, 2010, **8**, 31.
- 10 M. Lundqvist, J. Stigler, G. Elia, I. Lynch, T. Cedervall and K. A. Dawson, *Proc. Natl. Acad. Sci. U. S. A.*, 2008, **105**, 14265–14270.
- 11 S. Ritz, S. Schöttler, N. Kotman, G. Baier, A. Musyanovych, J. Kuharev, K. Landfester, H. Schild, O. Jahn, S. Tenzer and V. Mailänder, *Biomacromolecules*, 2015, **16**, 1311–1321.
- 12 S. Laurent, C. Burtea, C. Thirifays, F. Rezaee and M. Mahmoudi, *J. Colloid Interface Sci.*, 2013, **392**, 431–445.
- 13 M. J. Hajipour, S. Laurent, A. Aghaie, F. Rezaee and M. Mahmoudi, *Biomater. Sci.*, 2014, **2**, 1210–1221.
- 14 A. Lesniak, A. Campbell, M. P. Monopoli, I. Lynch, A. Salvati and K. A. Dawson, *Biomaterials*, 2010, **31**, 9511–9518.
- 15 S. Winzen, S. Schoettler, G. Baier, C. Rosenauer, V. Mailänder, K. Landfester and K. Mohr, *Nanoscale*, 2015, **7**, 2992–3001.
- 16 S. Schöttler, G. Becker, S. Winzen, T. Steinbach, K. Mohr, K. Landfester, V. Mailänder and F. R. Wurm, *Nat. Nanotechnol.*, 2016, DOI: 10.1038/NNANO.2015.330.
- 17 A. Lesniak, F. Fenaroli, M. P. Monopoli, C. Aberg, K. A. Dawson and A. Salvati, *ACS Nano*, 2012, **6**, 5845–5857.
- 18 E. Casals, T. Pfaller, A. Duschl, G. J. Oostingh and V. Puntes, *ACS Nano*, 2010, **4**, 3623–3632.
- 19 C. D. Walkey, J. B. Olsen, H. Guo, A. Emili and W. C. Chan, *J. Am. Chem. Soc.*, 2012, **134**, 2139–2147.
- 20 M. S. Ehrenberg, A. E. Friedman, J. N. Finkelstein, G. Oberdorster and J. L. McGrath, *Biomaterials*, 2009, **30**, 603–610.
- 21 T. M. Goppert and R. H. Muller, *Int. J. Pharm.*, 2005, **302**, 172–186.
- 22 M. P. Monopoli, D. Walczyk, A. Campbell, G. Elia, I. Lynch, F. B. Bombelli and K. A. Dawson, *J. Am. Chem. Soc.*, 2011, **133**, 2525–2534.
- 23 D. Baumann, D. Hofmann, S. Nullmeier, P. Panther, C. Dietze, A. Musyanovych, S. Ritz, K. Landfester and V. Mailänder, *Nanomedicine*, 2013, **8**, 699–713.
- 24 Z. Shriver, I. Capila, G. Venkataraman and R. Sasisekharan, *Handb. Exp. Pharmacol.*, 2012, 159–176, DOI: 10.1007/978-3-642-23056-1\_8.
- 25 S. A. Mousa and L. J. Petersen, *Thromb. Haemostasis*, 2009, **102**, 258–267.
- 26 R. J. Linhardt, *J. Med. Chem.*, 2003, **46**, 2551–2564.
- 27 O. Harush-Frenkel, N. Debotton, S. Benita and Y. Altschuler, *Biochem. Biophys. Res. Commun.*, 2007, **353**, 26–32.
- 28 S. E. A. Gratton, P. A. Ropp, P. D. Pohlhaus, J. C. Luft, V. J. Madden, M. E. Napier and J. M. DeSimone, *Proc. Natl. Acad. Sci. U. S. A.*, 2008, **105**, 11613–11618.
- 29 A. Verma and F. Stellacci, *Small*, 2010, **6**, 12–21.
- 30 H. P. Ekre, Y. Naparstek, O. Lider, P. Hyden, O. Hagermark, T. Nilsson, I. Vlodavsky and I. Cohen, *Adv. Exp. Med. Biol.*, 1992, **313**, 329–340.
- 31 K. T. Lappégard, M. Fung, G. Bergseth, J. Riesenfeld, J. D. Lambris, V. Videm and T. E. Mollnes, *Ann. Thorac. Surg.*, 2004, **77**, 932–941.
- 32 C. Passirani, G. Barratt, J. P. Devissaguet and D. Labarre, *Life Sci.*, 1998, **62**, 775–785.
- 33 M. Socha, A. Lamprecht, F. El Ghazouani, E. Emond, P. Maincent, J. Barre, M. Hoffman and N. Ubrich, *J. Nanosci. Nanotechnol.*, 2008, **8**, 2369–2376.
- 34 C. Passirani, G. Barratt, J. P. Devissaguet and D. Labarre, *Pharm. Res.*, 1998, **15**, 1046–1050.



35 M. Socha, P. Bartek, C. Passirani, A. Sapin, C. Damge, T. Lecompte, J. Barre, F. El Ghazouani and P. Maincent, *J. Drug Target.*, 2009, **17**, 575–585.

36 N. Jaulin, M. Appel, C. Passirani, G. Barratt and D. Labarre, *J. Drug Target.*, 2000, **8**, 165–172.

37 G. Baier, S. Winzen, C. Messerschmidt, D. Frank, M. Fichter, S. Gehring, V. Mailander and K. Landfester, *Macromol. Biosci.*, 2015, **15**, 765–776.

38 Y.-I. Chung, J. C. Kim, Y. H. Kim, G. Tae, S.-Y. Lee, K. Kim and I. C. Kwon, *J. Controlled Release*, 2010, **143**, 374–382.

39 I. Bleiberg, I. MacGregor and M. Aronson, *Thromb. Res.*, 1983, **29**, 53–61.

40 D. J. Falcone, *J. Cell. Physiol.*, 1989, **140**, 219–226.

41 G. Stehle, E. A. Friedrich, H. Sinn, A. Wunder, J. Harenberg, C. E. Dempfle, W. Maier-Borst and D. L. Heene, *J. Clin. Invest.*, 1992, **90**, 2110–2116.

42 K. A. Lindstedt, J. O. Kokkonen and P. T. Kovanen, *J. Lipid Res.*, 1992, **33**, 65–75.

43 A. Musyanovych, J. Dausend, M. Dass, P. Walther, V. Mailaender and K. Landfester, *Acta Biomater.*, 2011, **7**, 4160–4168.

44 D. Hofmann, S. Tenzer, M. B. Bannwarth, C. Messerschmidt, S.-F. Glaser, H. Schild, K. Landfester and V. Mailaender, *ACS Nano*, 2014, **8**, 10077–10088.

45 J. Patzig, O. Jahn, S. Tenzer, S. P. Wichert, P. de Monasterio-Schrader, S. Rosfa, J. Kuharev, K. Yan, I. Bormuth, J. Bremer, A. Aguzzi, F. Orfaniotou, D. Hesse, M. H. Schwab, W. Möbius, K. A. Nave and H. B. Werner, *J. Neurosci.*, 2011, **31**, 16369–16386.

46 R. A. Bradshaw, A. L. Burlingame, S. Carr and R. Aebersold, *Mol. Cell. Proteomics*, 2006, **5**, 787–788.

47 J. C. Silva, M. V. Gorenstein, G. Z. Li, J. P. Vissers and S. J. Geromanos, *Mol. Cell. Proteomics*, 2006, **5**, 144–156.

